Sequential *Cis/Trans* Autophosphorylation in TrkB Tyrosine Kinase

Yasuno Iwasaki, Hiroko Nishiyama, Kenji Suzuki, and Shinichi Koizumi*

Bio-Organic Research Department, International Research Laboratories, Ciba-Geigy (Japan) Limited, 10-66 Miyuki-cho, Takarazuka 665, Japan

Received August 15, 1996; Revised Manuscript Received December 20, 1996[⊗]

ABSTRACT: TrkB, a member of the tyrosine kinase family of growth factor receptors, is activated by binding of brain-derived neurotrophic factor or neurotrophin 4/5. The intracellular kinase domain of TrkB (ICD-TrkB) was prepared by an insect cell expression system and characterized to identify the mechanism of autophosphorylation. The time course of autophosphorylation, which shows a biphasic progression with a slow nonlinear phase followed by a fast linear phase, indicates the existence of autophosphorylation-induced activation in ICD-TrkB. This is also supported by the finding that phosphorylated ICD-TrkB shows significantly higher activity than control naive ICD-TrkB. Interestingly, the autophosphorylation rate in the linear phase clearly depends on the ICD-TrkB concentration, whereas the rate of initial autophosphorylation is independent of the concentration of ICD-TrkB in the reaction mixture. This observation suggests a two-step autophosphorylation, first an intramolecular activating step and then an intermolecular step. This mechanism is confirmed by the result that only the later phase of autophosphorylation is inhibited by addition of glycerol which interferes with intermolecular interactions. Therefore, we propose the mechanism of ICD-TrkB autophosphorylation as a sequential *cis/trans* phosphorylation.

Neurotrophins activate signal pathways that regulate cellular differentiation and survival in neurons. The neurotrophin family consists of nerve growth factor (NGF),[1] brain-derived neurotrophic factor (BDNF), neurotrophin-3 (NT-3), and neurotrophin-4/5 (NT-4/5) (Korsching, 1993; Lindsay et al., 1994). Members of the Trk family are the functional receptors of these neurotrophins and exhibit ligand selectivity. NGF preferentially binds to TrkA (Klein et al., 199; Kaplan et al., 1991); BDNF and NT-4/5 bind to TrkB (Soppet et al., 1991; Klein et al., 1991; Squinto et al., 1991; Berkemeier et al., 1991), and NT-3 binds to TrkC (Lamballe et al., 1991).

Trks are transmembrane glycoproteins and members of a receptor tyrosine kinase (RTK) family which includes insulin and epidermal growth factor receptors (IR and EGFR). Members of the RTK family have an extracellular ligand binding domain, a transmembrane domain, and an intracellular tyrosine kinase domain. The intracellular kinase domain is particularly well conserved in the RTK family (Hanks et al., 1988). The binding of ligand to the extracellular domain is thought to cause a conformational change of the receptor protein, leading to the autophosphorylation of specific tyrosine residues in the intracellular domain (Ullrich et al., 1990). For IR (Herrera et al., 1988; Villalba et al., 1989; Cobb et al., 1989; Li et al., 1992; Wei et al., 1995) and EGFR (Wedegaertner & Gill, 1989; Hsu et al., 1991; McGlynn et al., 1992; Cadena et al., 1994), extensive studies have been made on the enzymatic properties of tyrosine kinase using their intracellular domains prepared by an insect or mammalian cell expression system. These recombinant proteins show autophosphorylation activity without ligand simulation and also exhibit tyrosine kinase activity against exogenous peptides. The kinase activity for peptide substrates is extensively stimulated by autophosphorylation (Cobb et al., 1989; Wei et al., 1995; Hsu et al., 1991).

Autophosphorylated tyrosine residues in RTK are thought to contribute to the regulation of enzymatic activity and also to serve as the association sites with signal proteins containing Src homology 2 (SH2) domains (Pawson, 1995; Mayer & Baltimore, 1993), or phosphotyrosine binding (PTB) domains (Kavanaugh & Williams, 1994). Several tyrosine residues in the Trk family have been also reported to be autophosphorylated *in vivo* by ligand stimulation (Middlemas et al., 1994; Guiton et al., 1994) and *in vitro* (Loeb et al., 1994). Missense mutations of these tyrosine residues have revealed that some phosphotyrosines serve as binding sites for signaling proteins such as phospholipase C-γ (PLC-γ), phosphatidylinositol (PI-3) 3′-kinase and Shc (Loeb et al., 1994; Obermeier et al., 1993a,b, 1994; Stephens et al., 1994; Yao & Cooper, 1995). However, little is known about the mechanism by which the tyrosine kinase activity is regulated through the autophosphorylation.

To elucidate the nature of autophosphorylation events, we prepared the recombinant intracellular domain of TrkB (ICD-TrkB) with an insect cell expression system and characterized its autophosphorylation.

EXPERIMENTAL PROCEDURES

Materials. A mouse *trkB* cDNA was purchased from ATCC. pAcYM1 vector was kindly provided by Y. Matsuura (NIH, Japan). The Baculogold transfection kit was from PharMingen (San Diego, CA). Cell culture materials were from Gibco/BRL. *Spodoptera frugiperda* cells (Sf21) were generously provided by M. Summers (Texas A&M University) andmaintained in Grace's medium supplemented

* To whom correspondence should be addressed. Phone: 81-797-74-2625. Fax: 81-797-74-2455.

[⊗] Abstract published in *Advance ACS Abstracts,* February 15, 1997.

[1] Abbreviations: ICD-TrkB, intracellular kinase domain of TrkB; NGF, nerve growth factor; BDNF, brain-derived neurotrophic factor; NT, neurotrophin; IR, insulin receptor; EGF, epidermal growth factor; EGFR, EGF receptor; RTK, receptor tyrosine kinase; SH2, Src homology 2; PLC-γ1, phospholipase C-γ1; PI-3 kinase, phosphatidylinositol 3′-kinase; PY, phosphotyrosine; pICD-TrkB, phosphorylated ICD-TrkB; nICD-TrkB, nonphosphorylated ICD-TrkB.

S0006-2960(96)02057-0 CCC: $14.00

with 10% fetal calf serum according to a standard method by Summers and Smith (1987). Anti-phosphotyrosine (anti-PY) monoclonal antibody (4G10) was purchased from Upstate Biotechnology, Inc. (Lake Placid, NY). Horseradish peroxidase-conjugated anti-mouse and anti-rabbit IgG and the Enhanced Chemiluminescent (ECL) Detection Kit were from Amersham (Buckinghamshire, U.K.). Anti-pan-Trk antibody was from Santa Cruz Biotechnology, Inc. (Santa Cruz, CA). Anti-TrkB antibody was kindly provided by T. Mutoh (Fukui Medical School, Japan). Nitrocellulose was obtained from Bio-Rad. Butyl-Toyopearl was purchased from TOSOH (Tokyo, Japan). Mono Q (HR5/5), Superdex 75 HiLoad, and PD10 columns and Protein G-Sepharose beads were from Pharmacia/LKB. Centriprep 10 was from Amicon. [γ-^{32}P]ATP (3000 Ci/mmol) was from du Pont-NEN. Other reagents were of the highest grade available.

Construction of Recombinant Baculovirus. The cDNA fragment encoding a TrkB intracellular domain from Met-504 to Gly-821 was amplified from mouse *trkB* cDNA by PCR with oligonucleotide primers. A 5′ primer was 5′-GGATCCGACGCTGTCATTATTGGAATG-3′, and a 3′ primer was 5′-GGATCCGACGGTCTGGGCAGAAGGAG-GACC-3′, both having a new *Bam*HI site at their 5′ ends. The amplified fragment (2003−2978) was subcloned into a *Bam*HI site of the pAcYM1 vector. The recombinant baculovirus was constructed using the Baculogold transfection kit according to the manufacture's protocol and isolated by visual screening and dot blotting using anti-TrkB antibody.

Purification of ICD-TrkB from Insect Cells. The insect cells (1×10^9) were infected with the recombinant virus and cultured for 3 days suspended in 1 L of medium in a 5 L flask at 27 °C with continuous shaking. The cells were lysed by sonication in a buffer containing 50 mM Tris-HCl (pH 7.4), 1 mM phenylmethanesulfonyl fluoride, 10 μg/mL leupeptin, 10 μg/mL pepstatin, and 1 mM EDTA. After centrifugation at 10000*g* for 15 min, the supernatant was mixed with the same volume of 100% saturated ammonium sulfate solution (final 50% saturation), stirred on ice for 15 min, and then centrifuged at 10000*g* for 15 min. The precipitate was suspended in buffer A [440 mM ammonium sulfate, 20 mM Tris-HCl (pH 7.4), 1 mM EDTA, 10 μg/mL leupeptin, and 10 μg/mL pepstatin] and loaded onto a Butyl-Toyopearl column (5×10 cm) previously equilibriated in buffer A. The column was washed with buffer A and then eluted with a linear gradient of 440 to 0 mM ammonium sulfate of buffer A. The eluate, which contained ICD-TrkB, was pooled and precipitated with ammonium sulfate to a final concentration of 50% saturation. The precipitate was collected by centrifugation at 10000*g* for 15 min and dissolved in buffer B [50 mM MES-Na (pH 6.0), 1 mM EDTA, 10 μg/mL leupeptin, and 10 μg/mL pepstatin]. After being desalted with a PD10 column, the sample was loaded onto a Mono S (HR5/5) column equilibrated with buffer B, and the ICD-TrkB was eluted with a linear gradient of 0 to 0.5 M NaCl in buffer B. The pool of ICD-TrkB-containing fractions was concentrated by a Centriprep 10 concentrator and then subjected to a Superdex 75 HiLoad column previously equilibrated with buffer C [50 mM HEPES (pH 6.0), 150 mM NaCl, 0.1% Triton X-100, 1 mM EDTA, 10 μg/mL leupeptin, and 10 μg/mL pepstatin]. All purification procedures were done at 4 °C, and fractions from each purification step were analyzed by SDS/PAGE and Western blotting with anti-TrkB antibody as described in Autophosphorylation Assay. The protein concentration was determined with the BCA Protein Assay Reagent from Pierce (Rockford, IL) with bovine serum albumin as a standard. The final fraction containing ICD-TrkB was stored at −80 °C.

Autophosphorylation Assay. The standard reaction mixture contained 50 mM HEPES (pH 7.0), 0.1% Tween 20, 10 mM $MnCl_2$, 5 ng/μL ICD-TrkB, and the indicated concentration of ATP in a final volume of 20 μL. Reactions were carried out for 10 min or the indicated time at 30 °C and terminated by addition of 20 μL of 2× sampling buffer for SDS/PAGE. ICD-TrkB was resolved in SDS/PAGE with a 10% gel and then transferred onto a nitrocellulose membrane using a semidry electroblotting apparatus (Sartorius). The following immunostaining procedures were performed at room temperature. The membrane was blocked with 5% bovine serum albumin in TBSN [50 mM Tris-HCl (pH 7.4), 150 mM NaCl, and 0.2% Nonidet P-40] for 30 min and probed with 200 ng/mL anti-PY mAb for 1 h. After being washed with TBSN, the membrane was probed with peroxidase-conjugated anti-mouse IgG for 30 min. Then the membrane was washed again with TBSN and subjected to ECL detection as described in the manufacturer's protocol. The level of phosphorylation in ICD-TrkB was quantified with an image analyzer (Toyobo).

Analysis of the Reaction Rate with Different Concentrations of ICD-TrkB. To examine the effect of ICD-TrkB concentrations on the autophosphorylation rate, the standard assay was slightly modified. ICD-TrkB was autophosphorylated with 50 or 200 μM ATP with 4−16 ng/μL ICD-TrkB, and 10 ng of ICD-TrkB in each reaction was subjected to SDS/PAGE and analyzed by Western blotting using anti-PY antibody. For the experiment with a wide range of ICD-TrkB concentrations from 0.1 to 20 ng/μL, a step of immunoprecipitation was necessary before SDS/PAGE to concentrate ICD-TrkB. Autophosphorylation of ICD-TrkB (100 ng) with 50 μM ATP was performed in a different volume of reaction mixture to give the concentration of 0.1−20 ng/μL ICD-TrkB and was stopped by the addition of EDTA. Each sample was adjusted to give a final volume of 1 mL containing 50 mM EDTA, 50 mM HEPES (pH 7.0), and 0.1% Tween 20 and incubated for 1 h at 4 °C with 500 ng of anti-pan-Trk antibody. Then Protein G-Sepharose beads were added to the sample and incubated on a rotator for 1 h at 4 °C. After the beads were washed with TBSN three times, the immunoprecipitated ICD-TrkB was applied to SDS/PAGE and analyzed by Western blotting with anti-PY antibody. The recovery of ICD-TrkB was also examined by reprobing the blot with anti-pan-Trk antibody.

Phosphorylation of ICD-TrkB by Native and Autophosphorylation ICD-TrkB. To examine the effect of autophosphorylation on kinase activity, autophosphorylated and control naive ICD-TrkB (pICD-TrkB and nICD-TrkB) were prepared as follows; ICD-TrkB was incubated with (pICD-TrkB) or without (nICD-TrkB) 1 mM cold ATP in 50 mM HEPES (pH 7.0), 0.1% Tween 20, and 10 mM $MnCl_2$ for 40 min at 30 °C, and then ATP and $MnCl_2$ were removed by using a PD10 column equilibrated with 50 mM HEPES (pH 7.0) and 0.1% Tween 20. Phosphorylation of substrate ICD-TrkB (100 ng) for 5 min at 30 °C was carried out alone,

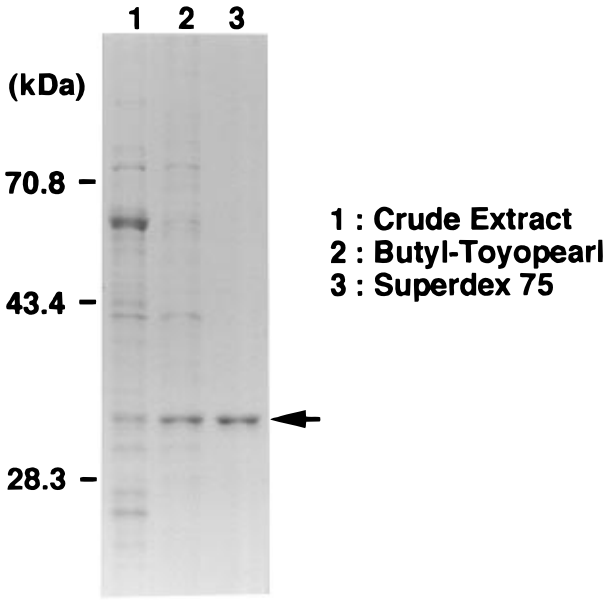

FIGURE 1: Purification of ICD-TrkB. Aliquots from the purification steps were analyzed by Coomassie blue staining after a 10% SDS/PAGE: lane 1, crude extract; lane 2, Butyl-Toyopearl pool; lane 3, Mono S pool; and lane 4, Superdex 75 pool.

or with pICD-TrkB (5 ng) or nICD-TrkB (5 ng), in a reaction mixture containing 20 μM ATP in the presence of 0.5 μCi/μL [γ-^{32}P]ATP. Samples were resolved on SDS/PAGE, and the incorporation of ^{32}P into ICD-TrkB was quantitated using a Fuji BAS-2000 photoimage analyzer.

RESULTS

Preparation of Recombinant ICD-TrkB with the Baculovirus Expression System. In order to examine the effect of receptor autophosphorylation on its tyrosine kinase activity, we expressed an intracellular kinase domain of TrkB (ICD-TrkB) in a *S. frugiperda* (Sf21) insect cell system. A ICD-TrkB recombinant virus was constructed to code for 318 amino acid residues from Met-504 to Gly-821. With anti-pan-Trk antibody, which recognizes a region on the carboxyl terminus of TrkB, ICD-TrkB was detected as a ~37 kDa protein in the lysates from Sf21 cells infected with recombinant virus (data not shown), which is consistent with the size predicted from the nucleotide sequence (M_r = 36 500 Da).

ICD-TrkB was purified from Sf21 cells infected with ICD-TrkB recombinant virus, using ammonium sulfate precipitation, Butyl-Toyopearl, Mono S, and Superdex 75 columns as described in Experimental Procedures. In the last step of purification, ICD-TrkB was eluted in a single peak from the Superdex 75 column at a position consistent with a 37 kDa monomer (data not shown). After four-step purification, ICD-TrkB was purified to homogeneity (Figure 1).

Detection of Tyrosine Kinase Activity of the Recombinant ICD-TrkB. The kinase activity of recombinant ICD-TrkB was confirmed by an autophosphorylation assay. Purified ICD-TrkB was incubated with ATP and $MnCl_2$, and autophosphorylation was quantified by Western blotting using anti-PY and anti-pan-Trk antibodies. As shown in Figure 2 (upper panel), ICD-TrkB was intensely autophosphorylated on tyrosine residues in the presence of ATP and $MnCl_2$. Phosphorylation of ICD-TrkB was associated with the shift of its mobility on SDS/PAGE (Figure 2, lower panel).

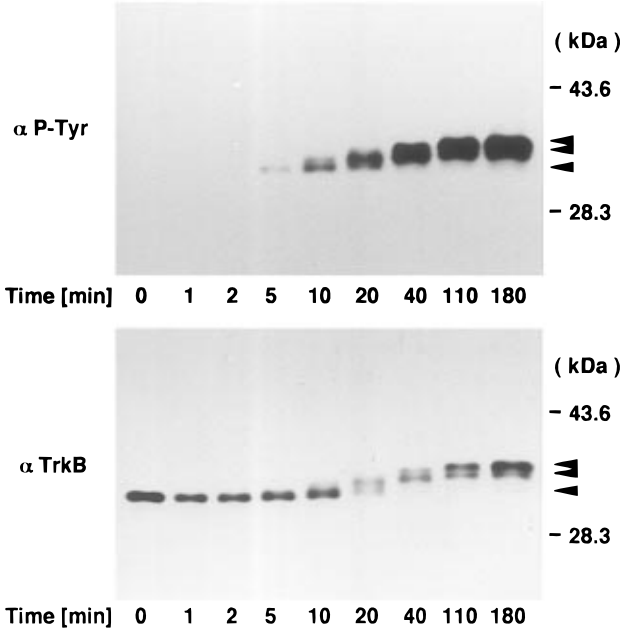

FIGURE 2: Autophosphorylation of ICD-TrkB. Purified ICD-TrkB (5 ng/μL) was incubated at 30 °C with 50 mM HEPES (pH 7.0), 0.1% Tween 20, 1 mM ATP, and 10 mM $MnCl_2$ for indicated periods. Phosphorylation of ICD-TrkB was detected by Western blotting using anti-PY (upper panel) and anti-pan-Trk (lower panel) antibodies as described in Experimental Procedures. Autophosphorylated ICD-TrkBs are indicated by arrow heads.

Because it has been reported that intracellular kinase domains of insulin and EGF receptors display a strong preference for Mn^{2+} rather than Mg^{2+} for autophosphorylation, the divalent metal ion requirement of ICD-TrkB was analyzed. Indeed, autophosphorylation of ICD-TrkB has a strong preference for Mn^{2+} over Mg^{2+} (Figure 3A). Additionally, the effect of ATP concentrations was examined, and the maximal autophosphorylation was observed at 2 mM ATP in 10 mM Mn^{2+}. The apparent K_m value for ATP was calculated as 160 μM (Figure 3B). This value is similar to the K_m reported for IR (Cobb et al., 1989) with peptide substrates but higher than that for EGFR (McGlynn et al., 1992). It is not simple to interpret this apparent K_m value obtained with ICD-TrkB, because the reaction associates with the conformational changes caused by multiple phosphorylation sites.

Activation of Tyrosine Kinase. The time course of autophosphorylation in ICD-TrkB was analyzed by Western blotting using anti-PY antibody and quantified (Figure 4). Autophosphorylation with 50 μM ATP presented a biphasic progression with a slow nonlinear phase followed by a fast linear phase, which suggests that an early phase of autophosphorylation activates ICD-TrkB. When the ATP concentration was increased to 200 μM, the time course of ICD-TrkB autophosphorylation displayed a linear increase without a detectable nonlinear phase.

To obtain direct evidence for the autophosphorylation-dependent activation of ICD-TrkB, the effect of autophosphorylation on its kinase activity was examined. ICD-TrkB was preincubated with 1 mM cold ATP (pICD-TrkB) or without ATP (nICD-TrkB) and then used as a catalyst for phosphorylation of substrate ICD-TrkB in the presence of [γ-^{32}P]ATP. This experiment was done on the basis of the model of *trans* autophosphorylation in the receptor kinase. As shown in Figure 5, a low level of ^{32}P incorporation was

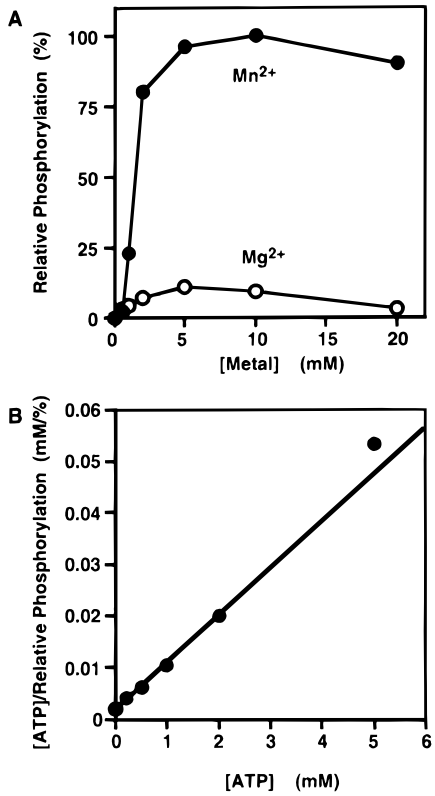

FIGURE 3: Kinetic properties. (A) Divalent metal ion requirement. Purified ICD-TrkB was autophosphorylated at 5 ng/μL of 1 mM ATP and indicated concentrations of $MnCl_2$ (●) or $MgCl_2$ (○). Phosphorylation of ICD-TrkB was measured as described in Experimental Procedures. A value of 100% was given to the activity measured at 10 mM $MnCl_2$. The same result was obtained in three separate experiments. (B) ATP requirement. Purified ICD-TrkB was autophosphorylated at 5 ng/μL with 10 mM $MnCl_2$ and indicated concentrations of ATP. Phosphorylation of ICD-TrkB was measured as described in Experimental Procedures. A value of 100% was given to the activity measured at 2 mM ATP. The results were plotted with a Hanes−Woolf plot, [ATP]/v vs [ATP]. The apparent K_m value of ICD-TrkB for ATP was calculated as 160 μM. The same result was obtained in three separate experiments.

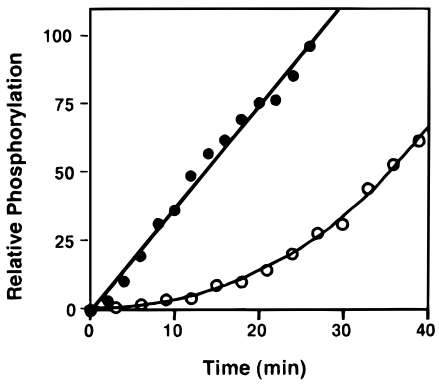

FIGURE 4: Time course analysis of autophosphorylation. Purified ICD-TrkB (5 ng/μL) was incubated with 50 (○) or 200 (●) μM ATP in the reaction mixture. Phosphorylation of ICD-TrkB was measured as described in Experimental Procedures. A value of 100% was given to the activity measured for 26 min with 200 μM ATP. The same result was obtained in three separate experiments.

observed after the incubation of substrate ICD-TrkB alone (lane 1). As previously demonstrated (Figure 3), ICD-TrkB shows low kinase activity in the presence of 20 μM ATP. The incubation of substrate ICD-TrkB with nICD-TrkB caused a small increase of ^{32}P incorporation (lane 2) when

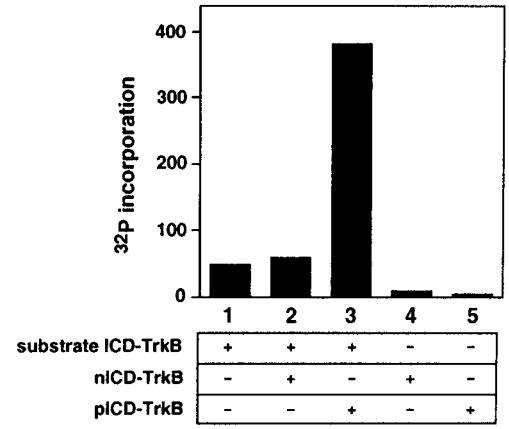

FIGURE 5: Stimulation of kinase activity by phosphorylation of ICD-TrkB. Autophosphorylated and control nonphosphorylated ICD-TrkB (pICD-TrkB and nICD-TrkB) were prepared by preincubation with or without 1 mM cold ATP as described in Experimental Procedures and used as a catalyst for the phosphorylation of substrate ICD-TrkB in the presence of [γ-^{32}P]ATP. Phosphorylation of substrate ICD-TrkB (100 ng) was carried out alone (lane 1) or with 5 ng of nICD-TrkB (lane 2) or pICD-TrkB (lane 3) for 5 min at 30 °C in the presence of 10 μM ATP containing 1 μCi [γ-^{32}P]ATP. nICD-TrkB (lane 4) and pICD-TrkB (lane 5) were also incubated alone in the same reaction conditions. Incorporation of ^{32}P into ICD-TrkB was quantitated using the Fuji BAS-2000 photoimage analyzer after SDS/PAGE. The same result was obtained in three separate experiments.

compared with that of the substrate ICD-TrkB alone (lane 1), according to the small increase of the ICD-TrkB concentration. In contrast, the incubation of substrate ICD-TrkB with pICD-TrkB caused a much bigger increase of ^{32}P incorporation (lane 3). Because little incorporation of ^{32}P was observed after the incubation of pICD-TrkB alone (lane 5), it was likely that the autophosphorylation of pICD-TrkB was saturated during the preincubation with cold 1 mM ATP. This shows that the substrate ICD-TrkB was extensively phosphorylated by the incubation with pICD-TrkB (lane 3). The phosphorylation observed in lane 3 may not be due solely to the activity of pICD-TrkB, because of a possible contribution of phosphorylated substrate ICD-TrkB. However, these experiments clearly indicate that the autophosphorylation of ICD-TrkB causes the activation of its kinase activity. Additionally, these results confirm that pICD-TrkB is able to phosphorylate other ICD-TrkB molecules intermolecularly.

Cis and Trans Phosphorylation. Whether receptor-type tyrosine kinases undergo *cis* or *trans* autophosphorylation has been the subject of recent debate. Our results demonstrated that the autophosphorylated ICD-TrkB is able to phosphorylate other molecules in a *trans* manner (Figure 5). However, the autophosphorylation of ICD-TrkB with 50 μM ATP exhibited two phases, nonlinear and linear (Figure 4). Thus, we characterized each phase to determine whether it is a *cis* or *trans* reaction. For this purpose, the rate of autophosphorylation was measured as a function of the concentration of ICD-TrkB. In the reaction with 200 μM ATP, the extent of phosphorylation per protein increased linearly with the concentration of ICD-TrkB (Figure 6A,B). When autophosphorylation was examined in the presence of 50 μM ATP, the extent of phosphorylation per protein also increased with the concentration of ICD-TrkB (Figure 6A,B). While these data suggest that the phosphorylation of ICD-TrkB occurs solely by *trans* phosphorylation, it was

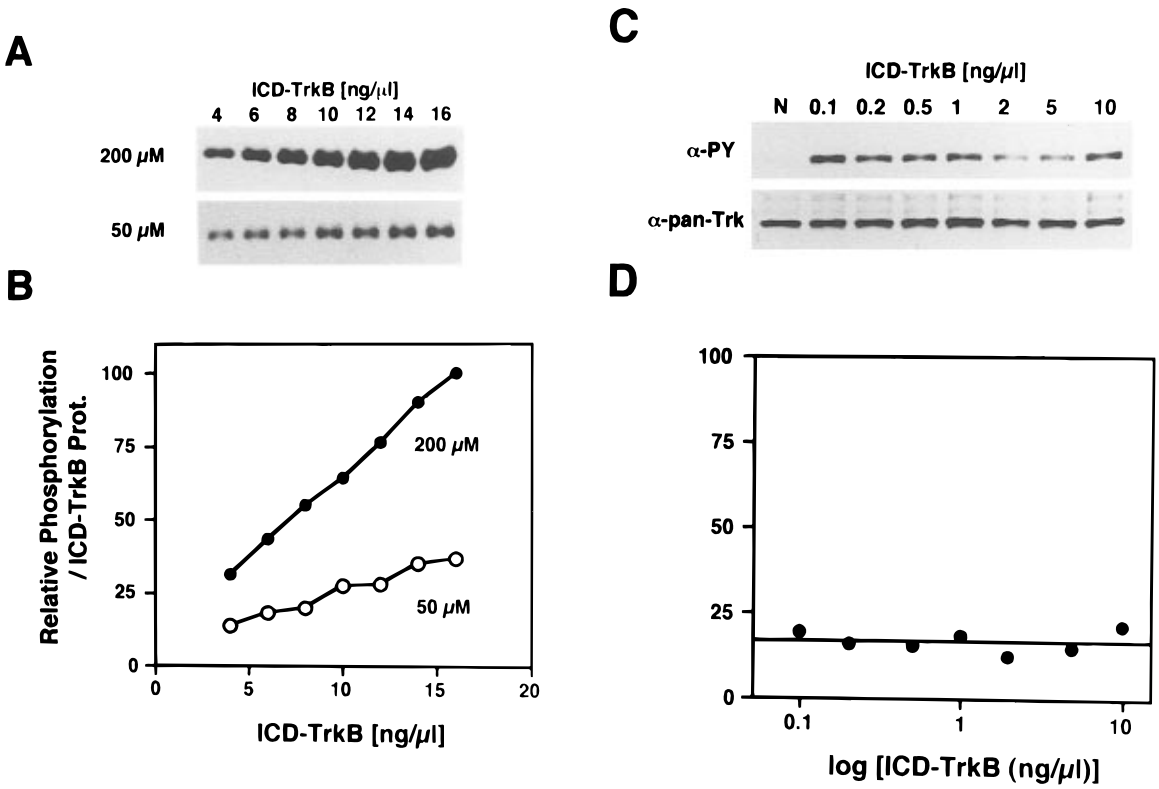

FIGURE 6: Effects of ICD-TrkB concentration on the rate of autophosphorylation. Autophosphorylation of ICD-TrkB with 50 (○) and 200 μM ATP (●) was detected by anti-PY blotting (A) and quantified (B) as described in Experimental Procedures. A value of 100% was given to the activity measured at 16 ng/μL with 200 μM ATP. Autophosphorylation with a wider range of ICD-TrkB concentrations was examined by addition of an immunoprecipitation step before SDS/PAGE. Phosphorylation and recovery in immunoprecipitants were analyzed by Western blotting using anti-PY and anti-pan-Trk antibodies (C) and quantified (D) as described in Experimental Procedures. Lane N in panel C indicates the recovery of ICD-TrkB at 0.1 μg/μL without phosphorylation. The phosphorylation does not affect the recovery of ICD-TrkB. The same result was obtained in three separate experiments.

possible that autophosphorylation is initially a *cis* phosphorylation event. To address this possibility, we then reexamined the earlier phase of autophosphorylation (5 min) at a much wider range of ICD-TrkB concentrations. For this experiment, an immunoprecipitation step was added before SDS/PAGE to concentrate and adjust the ICD-TrkB amount. Indeed, ICD-TrkB was quantitatively detected (Figure 6C), and it was found that the extent of phosphorylation per protein was obviously independent of the ICD-TrkB concentrations (Figure 6D). This indicates that the initial reaction in the nonlinear phase is intramolecular. As ICD-TrkB used in this study migrated as a monomeric form on gel filtration chromatography (data not shown), the intramolecular phosphorylation is considered to be a *cis* reaction. Therefore, a sequential *cis* and *trans* phosphorylation is suggested to take place in the autophosphorylation of ICD-TrkB.

Sequential Cis and Trans Phosphorylation. To demonstrate the sequential *cis* and *trans* phosphorylation directly, we carried out the autophosphorylation assay in the different concentrations of glycerol, which has been reported to interfere with intermolecular interaction by increasing viscosity. As the glycerol concentration was increased, the autophosphorylation of ICD-TrkB with 200 μM ATP was substantially inhibited, whereas the autophosphorylation with 50 μM ATP was not affected (Figure 7A,B). Furthermore, in a time course analysis of autophosphorylation with 50 μM ATP, the presence of 10% glycerol inhibited the later phase of the reaction but did not affect the initial phase (Figure 7C,D). These results provide additional evidence for the sequential *cis/trans* autophosphorylation of ICD-TrkB.

DISCUSSION

Ligand-induced autophosphorylation of receptor is considered to be a trigger of intracellular signal transduction. Whereas phosphorylation sites in the Trk family and their downstream signal cascades have been investigated extensively, their enzymatic properties as tyrosine kinase have not been studied. To understand the mechanism of Trk autophosphorylation, we expressed an intracellular domain of TrkB (ICD-TrkB) which contains the tyrosine kinase region and the potential autophosphorylation sites, using the baculovirus expression system. The recombinant ICD-TrkB was intensely autophosphorylated on multiple tyrosines in the presence of ATP and $MnCl_2$. The time course of autophosphorylation with 50 μM ATP, which shows a biphasic progression with a slow nonlinear phase followed by a fast linear phase, indicates that tyrosine kinase activity of ICD-TrkB is increased during autophosphorylation. This was also supported by the finding that phosphorylated ICD-TrkB showed significantly higher activity than control naive ICD-TrkB. Because the activation phase was not observed at a higher concentration of ATP, we can suppose that the mechanism of the autophosphorylation of ICD-TrkB increases its affinity to ATP so that the activation step is not necessary at the higher concentration of ATP. However, this does not rule out the possibility that the activation phase exists even at higher concentrations of ATP, but is very short. We are now examining the kinetic property of ICD-TrkB

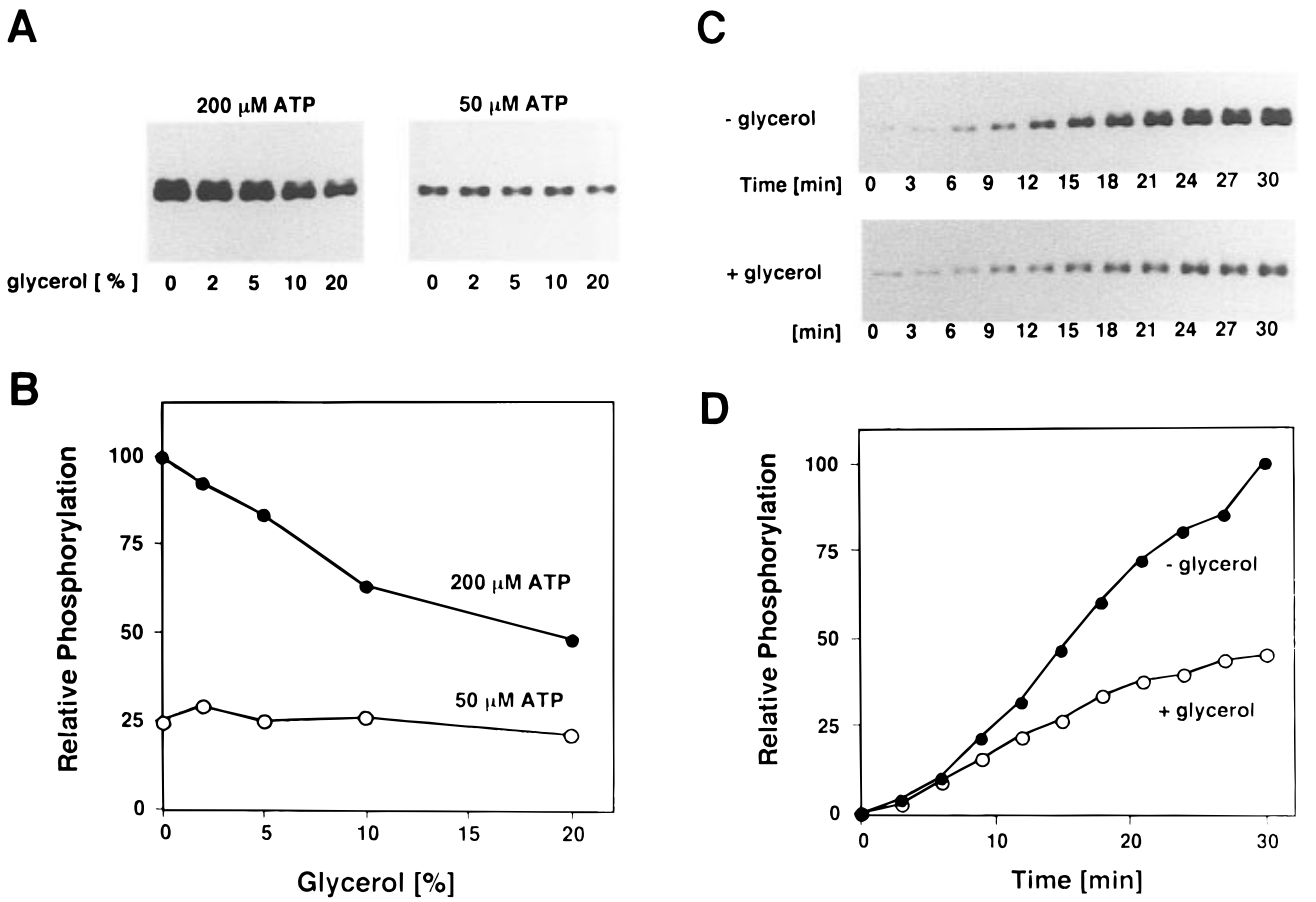

FIGURE 7: Effects of glycerol on the rate of autophosphorylation. (A and B) Effect of glycerol concentration on the autophosphorylation of ICD-TrkB. ICD-TrkB was autophosphorylated for 10 min in the presence of indicated concentrations of glycerol with 50 (○) and 200 (●) μM ATP and detected by Western blotting using anti-PY antibody (A), followed by quantification (B). A value of 100% was given to the activity measured with 200 μM ATP in the absence of glycerol. The same result was obtained in three separate experiments. (C and D) Effect of glycerol on the time course of autophosphorylation. ICD-TrkB was autophosphorylated with 50 μM ATP in the presence (○) or absence (●) of 10% glycerol and detected by Western blotting using anti-PY antibody (C), followed by quantification (D). A value of 100% was given to the activity measured for 30 min in the absence of glycerol. The same result was obtained in three separate experiments.

using exogenous substrates, which will provide important information about the activation mechanism.

Several tyrosines in TrkB have been reported to be autophosphorylated *in vivo* by ligand stimulation (Middlemas et al., 1994; Guiton et al., 1994). Peptide mapping analysis showed that these tyrosine residues in ICD-TrkB were all phosphorylated after *in vitro* autophosphorylation (I. Umemura, unpublished observations). Among these residues, Tyr-484, Tyr-751, and Tyr-785 are thought to serve as binding sites with particular signal proteins of Shc, PI-3 kinase, and PLC-γ, respectively. However, the function of phosphorylation of Tyr-670, Tyr-674, and Tyr-675, which are well conserved among the receptor kinase family, is not clear. Recently, Tyr-1015 in insulin receptor, which corresponds to Tyr-674 in TrkB, was reported to be involved in autoinhibition of kinase activity by binding to the active site (Hubbard et al., 1994). Therefore, Tyr-674 in TrkB is a possible site that regulates the kinase activity through its phosphorylation. Further experiments are necessary to confirm this.

In order to understand the mechanism of ligand-induced autophosphorylation in receptors, it is important to know whether the autophosphorylation takes place in a *cis* or *trans* manner. With the recombinant kinase domains of IR and EGFR, both *cis* (Villalba et al., 1989; Shoelson et al., 1991) and *trans* (Cobb et al., 1989; Wei et al., 1995; Treadway et al., 1991; Frattali et al., 1992; King et al., 1988; Honegger et al., 1990) mechanisms have been reported. Insulin hybrid receptors composed of a kinase inactive $\alpha\beta$-heterodimer and a COOH terminus-truncated $\alpha\beta$-heterodimer were shown to undergo *trans* autophosphorylation (Treadway et al., 1991; Frattali et al., 1992). Similar experiments support a *trans* phosphorylation mechanism for EGF receptor (King et al., 1988; Honegger et al., 1990). Furthermore, studies with a cytoplasmic kinase domain of insulin receptor are also consistent with the *trans* mechanism, which showed that the rate of autophosphorylation is dependent on enzyme concentration (Cobb et al., 1989; Wei et al., 1995). Other studies demonstrated a *cis* mechanism of autophosphorylation. When the cytoplasmic domain of the β subunit monomer of the insulin receptor was tested, autophosphorylation is not dependent on the enzyme concentration, suggesting that *cis* phosphorylation occurs in monomers (Villalba et al., 1989). Similar results were obtained using a trypsin-truncated insulin receptor which contained the whole β subunit and part of the α subunit (Shoelson et al., 1991). Recently, cotransfection experiments in COS-7 cells and fibroblasts showed that intermolecular phosphorylation of cytoplasmic domains occurred between TrkA or TrkB and their cognate chimeras (Canossa et al., 1996). However, this does not exclude *cis* phosphorylation of those receptors. Here we demonstrated that the autophosphorylation of ICD-TrkB shows two phases,

a nonlinear slow phase followed by a linear fast phase. Whereas the reaction in the linear phase mainly occurs by a *trans* mechanism, the initial reaction in the nonlinear phase occurs by a *cis* mechanism. This initial *cis* reaction would immediately be followed by *trans* phosphorylation. Because the change of phosphorylation mode from *cis* to *trans* is associated with the activation of kinase, *cis* phosphorylation is considered to be a key step of kinase activation in ICD-TrkB.

It seems to be quite reasonable that this sequential *cis*/*trans* autophosphorylation mechanism will apply to other receptor-type tyrosine kinases. Inconsistent results obtained in other studies with IR or EGFR are probably due to the difference of ATP concentrations in assays or due to differences in the degree to which the purified recombinant kinase had already been phosphorylated. On the basis of our observations and the previous results observed in insulin receptor (Hubbard et al., 1994), we suggest a mechanism in which a tyrosine residue interacting with the active site of the kinase is disengaged from the active site by *cis* phosphorylation and the active site becomes free and able to *trans* phosphorylate other molecules. Structural studies of ICD-TrkB and phosphorylated ICD-TrkB are necessary to confirm the mechanism suggested in this paper.

ACKNOWLEDGMENT

We thank Ms. M. Hashimoto for excellent assistance in the experiments and Dr. B. Goldsmith for helpful comments on the manuscript.

REFERENCES

Berkemeier, L. R., Winslow, J. W., Kaplan, D. R., Nikolics, K., Goeddel, D. V., & Rosenthal, A. (1991) *Neuron 7*, 857−866.
Cadena, D. L., Chan, C. L., & Gill, G. N. (1994) *J. Biol. Chem. 269*, 260−265.
Canossa, M., Rovelli, G., & Shooter, E. M. (1996) *J. Biol. Chem. 271*, 5812−5818.
Cobb, M. H., Sang, B. C., Gonzalez, R., Goldsmith, E., & Ellis, L. (1989) *J. Biol. Chem. 264*, 18701−18706.
Frattali, A. L., Treadway, J. L., & Pessin, J. E. (1992) *J. Biol. Chem. 267*, 19521−19528.
Guiton, M., Gunn-Moore, F. J., Stitt, T. N., Yancopoulos, G. D., & Tavare, J. M. (1994) *J. Biol. Chem. 269*, 30370−30377.
Hanks, S. K., Quinn, A. M., & Hunter, T. (1988) *Science 241*, 42−52.
Herrera, R., Lebwohl, D., Garcia de Herreros, A., Kallen, R. G., & Rosen, O. M. (1988) *J. Biol. Chem. 263*, 5560−5568.
Honegger, A. M., Schmidt, A., Ullrich, A., & Schlessinger, J. (1990) *Mol. Cell. Biol. 10*, 4035−4044.
Hsu, C. Y., Hurwitz, D. R., Mervic, M., & Zilberstein, A. (1991) *J. Biol. Chem. 266*, 603−608.
Hubbard, S. R., Wei, L., Ellis, L., & Hendrickson, W. A. (1994) *Nature 372*, 746−754.
Kaplan, D. R., Hempstead, B. L., Martin-Zanca, D., Chao, M. V., & Parada, L. F. (1991) *Science 252*, 554−558.
Kavanaugh, W. M., & Williams, L. T. (1994) *Science 266*, 1862−1865.
King, C. R., Borrello, I., Bellot, F., Comoglio, P., & Schlessinger, J. (1988) *EMBO J. 7*, 1647−1651.
Klein, R., Jing, S. Q., Nanduri, V., O'Rourke, E., & Barbacid, M. (1991a) *Cell 65*, 189−197.
Klein, R., Nanduri, V., Jing, S. A., Lamballe, F., Tapley, P., Bryant, S., Cordon-Cardo, C., Jones, K. R., Reichardt, L. F., & Barbacid, M. (1991b) *Cell 66*, 395−403.
Kohanski, R. A. (1993) *Biochemistry 32*, 5766−5772.
Korsching, S. (1993) *J. Neurosci. 13*, 2739−2748.
Lamballe, F., Klein, R., & Barbacid, M. (1991) *Cell 66*, 967−979.
Lee, J., O'Hare, T., Pilch, P. F., & Shoelson, S. E. (1993) *J. Biol. Chem. 268*, 4092−4098.
Li, S. L., Yan, P. F., Paz, I. B., & Fujita-Yamaguchi, Y. (1992) *Biochemistry 31*, 12455−12462.
Lindsay, R. M., Wiegand, S. J., Altar, C. A., & DiStefano, P. S. (1994) *Trends Neurosci. 17*, 182−190.
Loeb, D. M., Stephens, R. M., Copeland, T., Kaplan, D. R., & Greene, L. A. (1994) *J. Biol. Chem. 269*, 8901−8910.
Mayer, B. J., & Baltimore, D. (1993) *Trends Cell Biol. 3*, 8−13.
McGlynn, E., Becker, M., Mett, H., Reutener, S., Cozens, R., & Lydon, N. B. (1992) *Eur. J. Biochem. 207*, 265−275.
Middlemas, D. S., Meisenhelder, J., & Hunter, T. (1994) *J. Biol. Chem. 269*, 5458−5466.
Obermeier, A., Lammers, R., Wiesmuller, K. H., Jung, G., Schlessinger, J., & Ullrich, A. (1993a) *J. Biol. Chem. 268*, 22963−22966.
Obermeier, A., Halfter, H., Wiesmuller, K. H., Jung, G., Schlessinger, J., & Ullrich, A. (1993b) *EMBO J. 12*, 933−941.
Obermeier, A., Bradshaw, R. A., Seedorf, K., Choidas, A., Schlessinger, J., & Ullrich, A. (1994) *EMBO J. 13*, 1585−1590.
Pawson, T. (1995) *Nature 373*, 573−580.
Shoelson, S. E., Boni-Schnetzler, M., Pilch, P. F., & Kahn, C. R. (1991) *Biochemistry 30*, 7740−7746.
Soppet, D., Escandon, E., Maragos, J., Middlemas, D. S., Reid, S. W., Blair, J., Burton, L. E., Stanton, B. R., Kaplan, D. R., Hunter, T., Nikolics, K., & Parada, L. F. (1991) *Cell 65*, 895−903.
Squinto, S. P., Stitt, T. N., Aldrich, T. H., Davis, S., Bianco, S. M., Radziejewski, C., Glass, D. J., Masiakowski, P., Furth, M. E., Valenzuela, D. M., & DiStefano, P. S. (1991) *Cell 65*, 885−893.
Stephens, R. M., Loeb, D. M., Copeland, T. D., Pawson, T., Greene, L. A., & Kaplan, D. R. (1994) *Neuron 12*, 691−705.
Summers, M. D., & Smith, G. E. (1987) *A Manual of Methods for Baculovirus Vectors & Insect Cell Culture Procedures*, Bulletin no. 1555, Texas Agricultural Experiment Station.
Treadway, J. L., Morrison, B. D., Soos, M. A., Siddle, K., Olefsky, J., Ullrich, A., McClain, D. A., & Pessin, J. E. (1991) *Proc. Natl. Acad. Sci. U.S.A. 88*, 214−218.
Ullrich, A., & Schlessinger, J. (1990) *Cell 61*, 203−212.
Villalba, M., Wente, S. R., Russell, D. S., Ahn, J. C., Reichelderfer, C. F., & Rosen, O. M. (1989) *Proc. Natl. Acad. Sci. U.S.A. 86*, 7848−7852.
Wedegaertner, P. B., & Gill, G. N. (1989) *J. Biol. Chem. 264*, 11346−11353.
Wei, L., Hubbard, S. R., Hendrickson, W. A., & Ellis, L. (1995) *J. Biol. Chem. 270*, 8122−8130.
Yao, R., & Cooper, G. M. (1995) *Science 267*, 2003−2006.

BI962057X